Research Article

Green synthesized silver nanoparticles using aqueous leaf extracts of *Leucas aspera* exhibits antimicrobial and catalytic dye degradation properties

Muthusaravanan Sivaramakrishnan[1,2,3] · Vivek Jagadeesan Sharavanan[1,2,3] · Deenadayalan Karaiyagowder Govindarajan[1] · Yogesan Meganathan[1] · Bala Subramaniam Devaraj[1] · Sivarajasekar Natesan[2] · Ram Kothandan[3] · Kumaravel Kandaswamy[1]

Abstract

Green synthesis of silver nanoparticles (AgNPs) has been considered as a cost-effective and eco-friendly approach to generate a large volume of functionalized nanoparticles. In this work, AgNPs has been synthesized by reducing silver nitrate using an aqueous leaf extract of *Leucas aspera* (a medicinal plant found in Indian sub-continent) under ambient conditions. The UV/Vis peak at 428 nm confirmed the formation of AgNPs. FTIR (4500–750 cm^{-1}) analysis revealed the presence of bioactive functional groups coated over synthesized AgNPs. Furthermore, HR-TEM analysis of synthesized AgNPs confirmed the formation of nanostructures. The shape of the AgNPs was found to be spherical with sizes ranging from 20 to 40 nm. In addition, Face Centered Cubic structure of AgNPs was confirmed by XRD analysis. The antimicrobial effect of synthesized AgNPs was also studied in bacterial strains such as *Escherichia coli* (*E. coli*) and *Bacillus subtilis* (*B. subtilis*). The Minimal Inhibitory Concentration of AgNPs was found to be 30 µg/ml and 15 µg/ml for *B. Subtilis* and *E. coli*, respectively. In this study, we have also explored the synergistic effect of AgNPs conjugated with antibiotics such as Ampicillin and Kanamycin, results confirmed an increased antimicrobial activity against *E. coli* and *B. subtilis*. Finally, we have performed catalytic degradation of recalcitrant textile dyes using AgNPs and found that AgNPs were suitable for degradation of Optilan Red and Lanasyn Blue dyes.

Keywords Green synthesis · Characterization · Antibacterial · Synergistic effect · Catalytic degradation

Abbreviations

AgNPs	Silver nanoparticles
HR-TEM	High resolution Transmission Electron Microscopy
FTIR	Fourier Transform Infrared Spectroscopy
MIC	Minimum Inhibitory Concentration
ZOI	Zone of Inhibition
XRD	X Ray Diffraction analysis

1 Introduction

The green synthesized nanostructured materials have been critically acclaimed due to their unique physiochemical properties. In addition, green synthesis takes the advantage of biological systems such as plants [1], bacteria [2], yeast [3], fungi [4], and human cells [5]. Such biological systems possess an inherent ability to reduce inorganic metal ions into metal nanoparticles [6]. Furthermore, the green synthesis of nanoparticles are considered to be both cost-effective and eco-friendly in nature owing

✉ Kumaravel Kandaswamy, Kumaravel.k.bt@kct.ac.in | [1]Laboratory of Molecular Biology and Genetic Engineering, Department of Biotechnology, Kumaraguru College of Technology, Coimbatore, Tamil Nadu 641049, India. [2]Laboratory of Bioremediation Research, Department of Biotechnology, Kumaraguru College of Technology, Coimbatore, Tamil Nadu 641049, India. [3]Laboratory of Bioinformatics and Computational Biology, Department of Biotechnology, Kumaraguru College of Technology, Coimbatore, Tamil Nadu 641049, India.

SN Applied Sciences (2019) 1:208 | https://doi.org/10.1007/s42452-019-0221-1

Received: 19 November 2018 / Accepted: 26 January 2019 / Published online: 4 February 2019

to little or no release of harmful chemicals to the environment [7]. Therefore, in this study we took the advantage of aqueous leaf extracts of medicinal plant *Leucas aspera* (widespread throughout the Indian sub-continent from the northern Himalayas down to Ceylon also few parts of China and Bangladesh) to reduce silver nitrate into silver nanoparticles (AgNPs).

In this study we utilized *L. aspera* as a biological system of choice due to its ubiquitous in India and posses an antipyretic, anti-venom, antimicrobials, insecticide properties [8]. Previous studies on aqueous leaf extract of *L. aspera* have demonstrated the antibacterial effect of *L. aspera* extracts against *Vibrio cholerae, Escherichia coli, Salmonella typhi, Klebsiella aerogenes, Staphylococcus aureus, Proteus vulgaris*, and *Pseudomonas pyocyanea* [9]. Considering the antimicrobial potential of aqueous extract, in this study we synthesized AgNPs using *L. aspera* leaf extract as reducing and stabilizing agent and evaluated its antimicrobial activity.

The AgNPs can be functionalized using commercially available antibiotics such as glycosaminoglycans, making AgNPs a potent antimicrobial compound [10]. Recent studies on AgNPs conjugated with antibiotics demonstrates their ability to kill Gram-positive (*S. aureus*) and Gram-negative (*E. coli*) strain [11]. However, such conjugation method lacks precision and the precise molar concentration of antibiotics present on conjugated AgNPs was very difficult to regulate. In this study, we propose the use of AgNPs in combination with known concentration (20 µg/ml) of antibiotics such as Ampicillin and Kanamycin. Such synergistic approach increased the antimicrobial activity of AgNPs [12].

Besides being an antimicrobial compound, studies in the past demonstrates that green synthesized AgNPs also posses catalytic properties. For instance, green synthesized Zinc oxide (ZnO) nanoparticles using *Artocarpus heterophyllus* leaf extract possess the ability to degrade Rose Bengal dye from aqueous solution [13]. In addition, AgNPs synthesized using an aqueous solution of *Amaranthus gangeticus* were tested for their ability to degrade Congo red dye [14]. However, catalytic degradation of toxic textile dyes using AgNPs synthesized from *L. aspera* leaf extracts have not been reported till date. Therefore, in this study we explored the possibility of using green synthesized AgNPs in degrading recalcitrant textile dyes. Our results suggest that AgNPs were suitable for degradation of Optilan Red and Lanasyn Blue dyes. In essence, this study demonstrates the use of green synthesized AgNPs as a potent catalytic and antimicrobial agent.

2 Materials and methods

2.1 Methods

Silver nitrate ($AgNO_3$), Mueller–Hinton agar (MHA), Luria Broth, Kanamycin, Ampicillin were of analytical grade and purchased from Hi Media Pvt Ltd, India. Gram-negative *E. coli* (MTCC 443) and Gram-positive *B. subtilis* (MTCC 121) were obtained from MTCC, Chandigarh, India and used for antimicrobial studies.

2.2 Preparation of *Leucas aspera* extract

The leaf extract was prepared using the methods described in earlier publications [12]. The whole plant was collected from Sathyamangalam (southern part of India) forest area and used in this study. The collected plant sample was cleaned with deionized water to remove all dirt and allowed to shade dry to remove excess moisture content. The aqueous extract of *L. aspera* was prepared by heating 10 g of dried leaf sample in 100 mL of distilled water at 70 °C. The crude extract obtained was filtered through Whatman No. 1 filter paper. The leaf extracts were then sealed and stored at 4 °C for further analysis.

2.3 Green synthesis of silver nanoparticles

Green synthesis of nanoparticles was achieved using the methods described in previous publications with minor modification [1]. Green synthesis of AgNPs involves the reduction and stabilization of 0.1 M silver nitrate solution using *L. aspera* aqueous extract. Here, the plant extract functioned as a capping and reducing agent. Fifty milliliters of aqueous leaf extract added dropwise to 100 mL of 1 mM aqueous silver nitrate solution in Erlenmeyer flask with constant stirring at 500 rpm. The formation of AgNPs was identified by observing the color change from green to dark brown. The purification of AgNPs was performed by centrifugation at 15,000 rpm. The precipitate obtained was washed with ethanol three times to remove impurities and dried in an oven at 70 °C for 3–4 h. The synthesized AgNPs was stored in a brown bottle for characterization purpose.

2.4 Characterization of silver nanoparticles

The synthesized silver nanoparticles (AgNPs) were characterized by using UV/Vis spectroscopy, Fourier Transform Infrared Spectroscopy (FTIR), High-resolution Transmission Electron Microscopy (HRTEM) and X-Ray Diffraction (XRD). The Reduction of $AgNO_3$ into AgNPs with the addition of

aqueous plant extract was identified by the formation of surface Plasmon resonance peak (~400 nm) using UV/Vis spectroscopy. The FTIR (at 4500–750 cm^{-1}) analysis was performed for identification of various bioactive functional groups present in aqueous plant extract and coated over synthesized AgNPs during reduction and stabilization process. The XRD analysis was performed to determine the structure, phase purity, lattice parameters of synthesized AgNPs. HRTEM was performed to determine the size, morphology, and agglomeration of AgNPs.

2.5 Antibacterial activity of the synthesized AgNPs from *Leucas aspera*

The antibacterial activity of the synthesized AgNPs was determined by well diffusion method against *E. coli* (MTCC 443) and *B. subtilis* (MTCC 121). The strains were cultivated in Luria broth at 37 °C for 18 h and used for bacterial studies.

2.6 Well diffusion assay

The well diffusion is a standard method for antibacterial evaluation of metal nanoparticles [15]. The bacterial subcultures were standardized to 0.5 McFarland standard and seeded to MHA agar under the biosafety hood. Four wells each of 6 mm was made on MHA agar using a sterile gel puncture syringe and labeled. The aqueous solution of AgNPs of different concentrations (50, 75 and 100 µg/ml) was prepared and loaded into each well and penicillin was used as the positive control. The Zone of Inhibition (ZOI) was measured from MHC agar plates after 24 h at 37 °C. The experiments were performed in triplicates and the percentage of inhibition was calculated using the formula.

$$\text{Inhibition percentage}\ (\%) = \left(\left(\text{ZOI}_{\text{AgNPs}} - \text{ZOI}_{\text{control}}\right) \times 100\right) / \text{ZOI}_{\text{control}} \quad (1)$$

2.7 Minimum inhibitory concentration of synthesized AgNPs

The Minimum Inhibitory Concentration **(**MIC) assay was performed as described in the earlier publications [16] with slight modifications. Top layer agar plates containing lawns of *E. coli* (MTCC 443) and *B. subtilis* (MTCC 121) were prepared by mixing 5 mL of LB broth containing 0.8% agar and 1 mL of overnight cultures. The mixture was then poured onto LB agar plates and allowed to solidify for 15 min and 10 µL of this serially diluted AgNPs was then added to the top layer of agar plates containing lawns of the appropriate strain. The plates were incubated overnight for 18 h at 37 °C and colonies were observed to determine the MIC.

2.8 Synergistic effect with antibiotics

To evaluate the synergistic effect of the obtained AgNPs with antibiotics, the bacterial cultures were standardized to 0.5 McFarland standard and seeded to MHA agar under the biosafety hood. The 20 µg/ml stock solution of both AgNPs and antibiotics were prepared, mixed well and 10 µl of AgNPs-antibiotics mixtures were loaded to the respective wells and antibiotics were used as a controls. Incubate the loaded MHC agar plates at 37 °C for 24 h and measured the *ZOI*. The experiments were performed triplicates and Mean inhibition zone diameter was calculated. The Synergistic effect of antibiotic with AgNPs addition was calculated as follows

$$\textit{Increase in fold percentage}\ (\%) = \frac{b-a}{a} \times 100 \quad (2)$$

$$\textit{Increase in fold area}\ (\textit{sq.mm}) = \frac{b^2 - a^2}{a^2} \quad (3)$$

where a is *ZOI* of Antibiotics alone and b is *ZOI* of Antibiotics and AgNPs combination.

2.9 Dye degradation study

The catalytic of dye degradation activity of the synthesized AgNPs were performed as described in the previous publication [17] with minor modification. A 500 µL of AgNPs (in varying concentrations of 62.5, 125 and 250 µg/mL) were prepared and added to 2.5 mL of dye solution (50 µg/mL) and incubated for 45 min at 35 °C. Further, the sample was centrifuged was centrifuged at 15,000 rpm to remove AgNPs. The dye solution was diluted 20 fold and measured for absorbance at corresponding λ_{max}. The degradation of dye was observed by decreasing in absorbance value due to decolourisation of dye solution. The dye degradation percentage was calculated as described [18],

$$\textit{Degradation percentage} = \frac{\text{Initial absorbance of the dye} - \text{Final absorbance of the dye}}{\text{Initial absorbance of the dye}} \times 100 \quad (4)$$

3 Results and discussion

3.1 Green synthesis and characterization of AgNPs

The Biogenic reduction of silver nitrate with *L. aspera* leaf extract results in the formation of AgNPs, which was confirmed by the appearance of dark brown color after overnight incubation. The color change acts as the preliminary steps to predict the formation of nanoparticles [19].

3.2 UV–Vis spectroscopy and FTIR analysis

The reduction of $AgNO_3$ into silver nanoparticle with the addition of aqueous plant extract was identified by the formation of surface plasmon resonance peak at 428 nm using UV–Vis spectroscopy. Figure 1 shows the UV–Vis spectrum of AgNPs synthesized using *L. aspera* aqueous extract showing surface plasmon resonance peak at 428 nm that confirms the presence of AgNPs. Studies on green synthesis of AgNPs suggest that the biogenic reduction of $AgNO_3$ with plant extracts was due to various bioactive functional groups present in aqueous plant extract [20], which coated over synthesized AgNPs during reduction and stabilization process.

The FTIR spectroscopy was performed for both leaf extract and synthesized nanoparticles and illustrated in Fig. 2. The FTIR spectrum of *L. aspera* leaf extract and synthesized AgNPs shows a shift in peaks at range 3420–3371 (due to N–H stretching, amides), 1635–1650 (due to C=O stretching, amides) and 1000–1320 cm^{-1} (characteristic of a C–O stretch, Carboxylic acids). Apart from that synthesized AgNPs shows peaks at 1826, 1521, 1247 cm^{-1} related to C=O stretching, N–O stretching of aromatic nitro compounds and

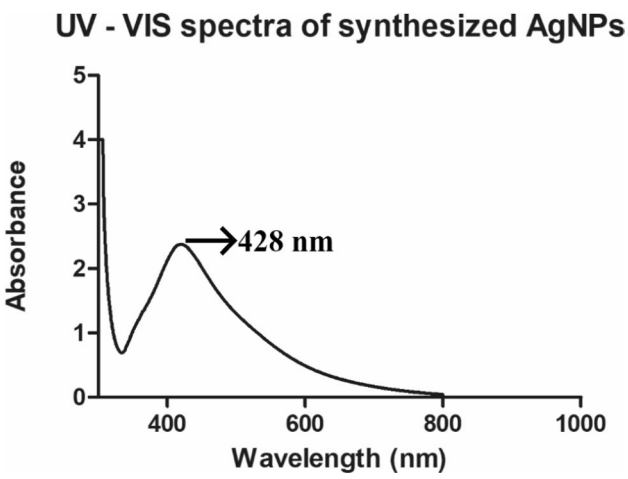

Fig. 1 UV–Vis spectra of AgNPs synthesized using *Leucas aspera* aqueous extract showing surface plasmon resonance peak at 428 nm

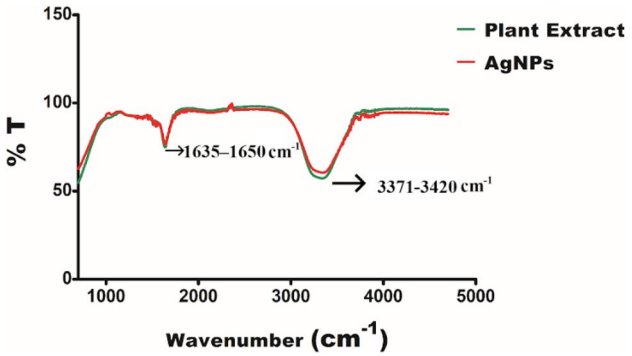

Fig. 2 FTIR spectra of *Leucas aspera* aqueous extract and green synthesized AgNPs

C–N stretching aromatic amine respectively. The surface of AgNPs contains functional groups corresponding to amides, nitro compounds and carboxylic acid. The polyphenols and proteins present in the *L. aspera* could act as both reducing and encapsulated agents and aids the reduction of $AgNO_3$ to AgNPs. The opto-electric spectrum analysis using UV/Vis spectroscopy and FTIR spectroscopy only explains the formation and surface functional groups of the synthesized AgNPs.

3.3 HR-TEM analysis

HR-TEM was performed to investigate the size and morphology of the AgNPs. Samples were prepared as per the protocol and coated over the copper grids and the particle size was evaluated using Fiji software. Figure 3 shows HRTEM micrographs of synthesized AgNPs which confirms the formation of nanostructures. The Silver nanoparticles produced by the green synthesis method shows uniformity in the shape as most are spherical in shape and the image shows that the particles produced are monodispersed (Fig. 3a). The magnified image (Fig. 3b) clearly shows the fringes which shows the orderly arrangement of the atoms in the nanoparticles. The shape of the most AgNPs was found to be spherical and the particle size ranges from 20 to 40 nm.

3.4 XRD analysis

The XRD pattern of dried AgNPs was shown in Fig. 4. The XRD shows peaks at 39°, 44.5°, 65°, 77° and 82° which correspond to {1,1,1},{2,0,0},{2,2,0},{3,1,1} and {2,2,2} crystalline planes which confirms the face centered cubic crystalline (according to standard Joint Committee for Powder Diffraction Set, # 89-3722) structure of synthesized AgNPs and the sharpness of peaks indicates the particles are in the nano range. The other smaller peaks visible in the graph are due to the unreacted silver nitrate in the

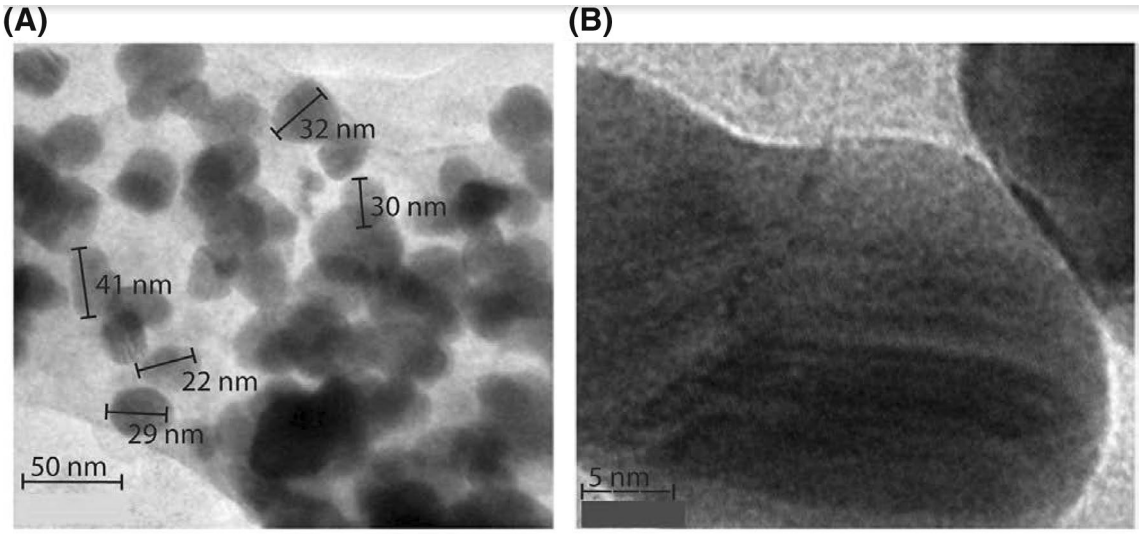

Fig. 3 HRTEM micrograph images of AgNPs synthesized using leaf extract of *Leucas aspera* showing the spherical shaped particle of size ranges from 20 to 40 nm. **a** Diameter of five spherical AgNPs were measured and **b** fringes in AgNPs indicating orderly arrangement of the atoms, scale bar 5 nm

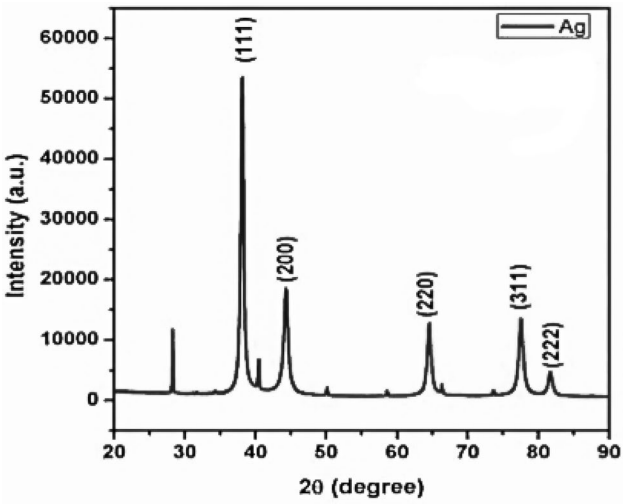

Fig. 4 XRD pattern of AgNPs synthesized using *Leucas aspera* leaf extract

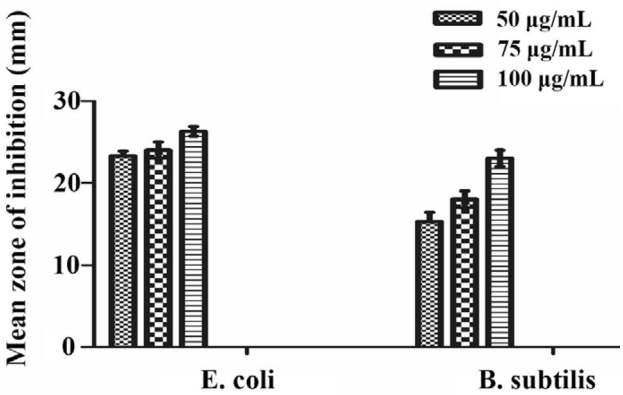

Fig. 5 Antibacterial activity of AgNPs synthesized using *Leucas aspera* leaf extract

solution of the nanoparticles. The broadness of the peaks indicates the small size of the particles synthesized [21].

3.5 The antibacterial and synergistic effect of AgNPs

The synthesized AgNPs shows antibacterial activity against *E. coli* (MTCC 443) and *B. subtilis* (MTCC 121). A varying concentrations of synthesized AgNPs were diluted and tested for antibacterial activity against the aforementioned strains and antibacterial activity was evaluated based on the *ZOI*. It is found that the *ZOI* increases with increases in AgNPs concentration. The AgNPs of different concentrations (50, 75 and 100 µg/ml) were prepared and added into the wells on MHA plate containing bacterial culture and *ZOI* was measured after the incubation period of 24 h and results were illustrated in Fig. 5. Table 1 shows the effect of varying concentrations of AgNPs on *E. coli* and *B. subtilis*. The *ZOI* was found to be 23.3 ± 0.58, 24 ± 1 and 26.3 ± 0.58 mm against Gram-Negative *E. coli* for AgNPs concentrations of 50, 75 and 100 µg/mL respectively. For Gram-Positive *B. subtilis,* the *ZOI* was found to be 15.30 ± 1.15, 18 ± 1, 23 ± 1 for the same AgNPs concentration range. The Inhibition percentage was calculated using Eq. (1). The MIC for *L. aspera* capped AgNPs was estimated to be 30 µg/ml and 15 µg/ml for *B. Subtilis* and *E. coli*, respectively. The results for top layer agar plates assay

Table 1 Effect of different concentration of *Leucas aspera* leaf extract reduced AgNPs on *Escherichia coli* and *Bacillus subtilis*

Concentration of AgNPs (µg/ml)	*Escherichia coli*			*Bacillus subtilis*		
	50	75	100	50	75	100
Zone of inhibition (mm)	23.3 ± 0.58	24 ± 1	26.3 ± 0.58	15.30 ± 1.15	18 ± 1	23 ± 1
Inhibition percentage (%)[a]	94.16	100	100	27.5	50	91.6

[a]The inhibition percentage was calculated with respect to Ampicillin (as control)

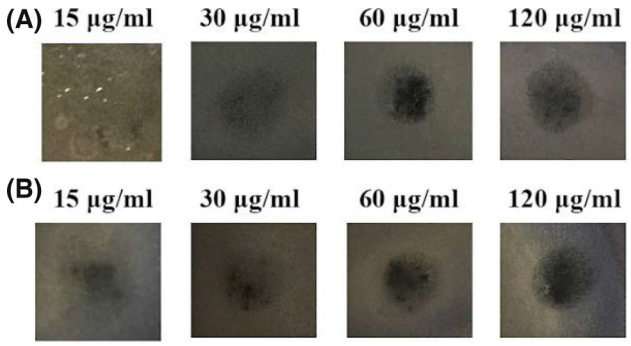

Fig. 6 Minimum inhibitory concentration of AgNPs synthesized using *Leucas aspera* leaf extract for **a** *B. Subtilis* and **b** *E. Coli*

was given in Fig. 6. Table 2 shows the synergistic effect of AgNPs with common antibiotics such as Ampicillin and Kanamycin against *E. coli* and *B. subtilis*. To quantify the synergistic effect of AgNPs, the increase in *ZOI* was estimated in terms of area and percentage using the Eqs. (2) and (3). Ampicillin shows maximum synergistic effect with AgNPs against both *E. coli* and *B. subtilis* than the Kanamycin (Table 2). Figure 7 shows the synergistic effect of AgNPs with Amplicillin and Kanamycin on *E. coli* and *B. subtilis*. The synthesized AgNPs shows maximum antibacterial activity against the gram-negative bacteria, owing to the difference in cell membrane architecture. The cell membrane of gram-negative bacteria composed of thin peptidoglycan layer and a thin exterior layer of liposaccharides which has negative electrostatic charges that attract and assists diffusion of positively charged AgNPs inside the cell wall. But Gram-positive bacteria have a thick peptidoglycan layer composed of teichoic acids and shows resistant to AgNPs. The antibiotics contain various functionally active groups, which may react with the nanoparticle by chelation or binding of antibiotics and nanoparticles through van der Waals interaction that results in antibiotics-AgNPs complex. The AgNPs acts as the drug delivery vehicle that facilitates the antibiotics to reach cell interior and increase the possibility of drug-target interaction. The AgNPs facilitates the targeted delivery of the hydrophilic drug through the hydrophobic bacterial membrane architecture. In addition, the surface of green synthesized AgNPs contains functional groups corresponding to amides, nitro compounds, a carboxylic acid which also contributes antibacterial activity.

3.6 Catalytic dye degradation property of AgNPs

In this work, the dye degradation properties of *L. aspera* caped silver nanoparticles were tested for textile dyes Optilan Red and Lanasyn Blue. The absorbance maximum

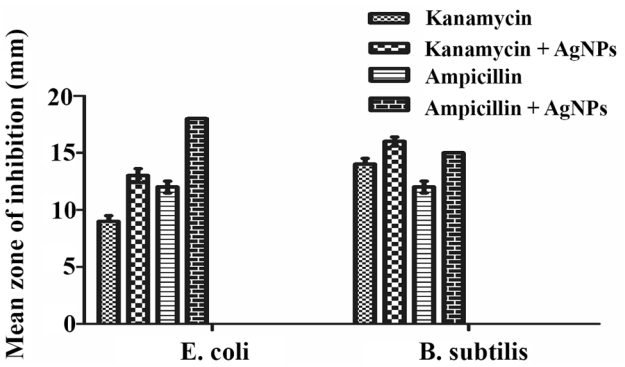

Fig. 7 Synergistic antibacterial activity of AgNPs synthesized using *Leucas aspera* leaf extract with common antibiotics

Table 2 Synergistic effect of *Leucas aspera* leaf extract reduced AgNPs with common antibiotics on *Escherichia coli* and *Bacillus subtilis*

Bacterial strains	Commercial antibiotics	Mean zone of inhibition (mm) with antibiotics	Mean zone of inhibition (mm) AgNPs with antibiotics	Increase in fold area (mm^2)	Increase in percentage (%)
Escherichia coli	Kanamycin	9	13	1.086	44.44
	Ampicillin	12	18	1.25	50
Bacillus subtilis	Kanamycin	14	16	0.306	14.28
	Ampicillin	12	15	0.56	25

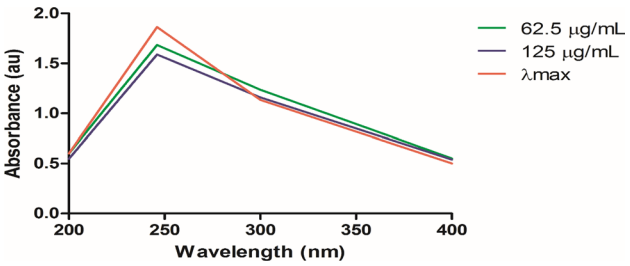

Fig. 8 Overlay UV–Vis spectra of Optilan red degradation in presence of AgNPs using *Leucas aspera* leaf extract

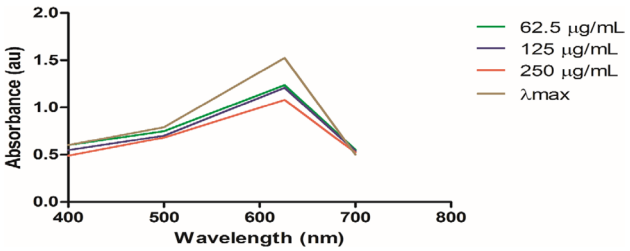

Fig. 9 Overlay UV–Vis spectra of Lanasyn Blue degradation in presence of AgNPs using *Leucas aspera* leaf extract

(λ_{max}) of Optilan Red and Lanasyn Blue dyes were found to be 246 nm, 626 nm using UV–Vis spectroscopy analysis. The dye degradation reactions were conducted in test tubes for 45 min at 35 °C with addition of varying concentration of green synthesized AgNPs and degree of decolourization was observed using UV–Vis spectrophotometer [22]. The dye degradation percentage of Lanasyn Blue was found to be 9.6%, 14.75% for AgNPs concentrations of 62.5, 125 µg/mL respectively. Figure 8 shows the Overlay UV spectra for degradation of Lanasyn Blue in presence of varying concentration of *L. aspera* leaf extract capped AgNPs. For Optilan Red dye, the degradation percentage was found to be 18.89, 20.80, 29.19% for the AgNPs concentrations of 62.5, 125, 250 and 125 µg/mL, respectively. Figure 9 illustrates the Overlay UV spectra for Optilan Red dye degradation in presence of varying concentration of *L. aspera* leaf extract capped AgNPs.

4 Conclusion

This study demonstrates the potential of AgNPs produced from *L. aspera* as an active catalytic and antimicrobial agent. Our green sythesis approach takes advantage of leaf extract from medicinal plant (*L. aspera*) that eliminates the need for toxic chemical reducing agents. The green synthesized AgNPs used in this study also posses dye degradation properties. In addition, the synergitic approach of combining AgNPs with antibiotics further enhances the antimicrobial propertis of green synthesized AgNPs. In summary, this study could possibly pave a way for large scale green synthesis of AgNPs that posses dual (antimicrobial and dye degradation) properties.

Acknowledgements The authors gratefully acknowledge Department of Biotechnology, Kumaraguru College of Technology (KCT), Coimbatore, Tamil Nadu, India for providing us the research facilities.

Compliance with ethical standards

Conflict of interest The authors report no conflict of interest.

References

1. Mittal AK, Chisti Y, Banerjee UC (2013) Synthesis of metallic nanoparticles using plant extracts. Biotechnol Adv 31(2):346–356
2. Saifuddin N, Wong CW, Yasumira AAN (2009) Rapid biosynthesis of silver nanoparticles using culture supernatant of bacteria with microwave irradiation. J Chem 6(1):61–70
3. Sharma VK, Yngard RA, Lin Y (2009) Silver nanoparticles: green synthesis and their antimicrobial activities. Adv Colloid Interface Sci 145(1–2):83–96
4. Li G, He D, Qian Y, Guan B, Gao S, Cui Y, Yokoyama K, Wang L (2012) Fungus-mediated green synthesis of silver nanoparticles using Aspergillus terreus. Int J Mol Sci 13(1):466–476
5. Venil CK, Sathishkumar P, Malathi M, Usha R, Jayakumar R, Yusoff ARM, Ahmad WA (2016) Synthesis of flexirubin-mediated silver nanoparticles using *Chryseobacterium artocarpi* CECT 8497 and investigation of its anticancer activity. Mater Sci Eng, C 59:228–234
6. Vaidyanathan R, Kalishwaralal K, Gopalram S, Gurunathan S (2009) Enhanced silver nanoparticle synthesis by optimization of nitrate reductase activity. Biotechnol Adv 75(1):335–341
7. Francis S, Joseph S, Koshy EP, Mathew B (2018) Microwave assisted green synthesis of silver nanoparticles using leaf extract of elephantopus scaber and its environmental and biological applications. Artif Cells Nanomed Biotechnol 46(4):795–804
8. Srinivasan R, Ravali B, Suvarchala P, Honey A, Tejaswini A, Neeraja P (2011) *Leucas aspera*-medicinal plant: a review. Int J Pharma Bio Sci 4(12):4777–4779
9. Shah M, Prajapati M, Patel J, Modi K (2010) *Leucas aspera*: a review. Pharmacogn Rev 4(7):85
10. Kemp MM, Kumar A, Mousa S, Park TJ, Ajayan P, Kubotera N, Mousa SA, Linhardt RJ (2009) Synthesis of gold and silver nanoparticles stabilized with glycosaminoglycans having distinctive biological activities. Biomacromol 10(3):589–595
11. Rai A, Prabhune A, Perry CC (2010) Antibiotic mediated synthesis of gold nanoparticles with potent antimicrobial activity and their application in antimicrobial coatings. J Mater Chem 20(32):6789–6798
12. Krishna G, Kumar SS, Pranitha V, Alha M, Charaya S (2015) Biogenic synthesis of silver nanoparticles and their synergistic effect with antibiotics: a study against salmonella SP. Int J Pharm Pharm Sci 7(11):84–88
13. Vidya C, Prabha MNC, Raj MALA (2016) Green mediated synthesis of zinc oxide nanoparticles for the photocatalytic degradation of Rose Bengal dye. Environ Nanotechnol Monit Manag 6:134–138

14. Kolya H, Maiti P, Pandey A, Tripathy T (2015) Green synthesis of silver nanoparticles with antimicrobial and azo dye (Congo red) degradation properties using *Amaranthus gangeticus* Linn leaf extract. J Anal Sci Technol 6(1):33
15. Bauer AW, Kirby WM, Sherris JC, Turck M (1966) Antibiotic susceptibility testing by a standardized single disk method. Am J Clin Pathol 45:493–496
16. Kandaswamy K, Horng T, Wang CY, Huston-warren E, Meyerhoffert U (2013) Focal targeting by human β-defensin 2 disrupts localized virulence factor assembly sites in Enterococcus faecalis. Proc Natl Acad Sci 110(50):20230–20235
17. Sharma P, Pant S, Poonia P, Kumari S, Dave V, Sharma S (2018) Green synthesis of colloidal copper nanoparticles capped with *Tinospora cordifolia* and its application in catalytic degradation in textile dye: an ecologically sound approach. J Inorg Organomet Polym Mater 28:2463
18. Sivarajasekar N, Mohanraj N, Sivamani S, Ganesh Moorthy I, Kothandan R, Muthusaravanan S (2018) Comparative modeling of fluoride biosorption onto waste Gossypium hirsutum seed microwave-bichar using response surface methodology and artificial neural networks. IEEE Xplore 17:1631–1635
19. Mochochoko T, Oluwafemi OS, Jumbam DN, Songca SP (2013) Green synthesis of silver nanoparticles using cellulose extracted from an aquatic weed; water hyacinth. Carbohydr Polym 98(1):290–294
20. Li S, Shen Y, Xie A, Yu X, Qiu L, Zhang L, Zhang Q (2007) Green synthesis of silver nanoparticles using *Capsicum annuum* L. extract. Green Chem 9(8):852–858
21. Khlebtsov NG (2008) Determination of size and concentration of gold nanoparticles from extinction spectra. Anal Chem 80(17):6620–6625
22. Jyoti K, Singh A (2016) Green synthesis of nanostructured silver particles and their catalytic application in dye degradation. J Genet Eng Biotechnol 15(1):31–39